Desalination and Water Treatment
www.deswater.com
doi: 10.5004/dwt.2020.25066

180 (2020) 219–226
March

Preparation of a novel inorganic-biological composite flocculant for the removal of turbidity and organic matter in the surface water

Lixin Li[a,b,c,*], Yongjian Piao[b], Fang Ma[c,*], Tao Sheng[a], Caiyu Sun[a], Wanmeng Liu[a]

[a]*School of Environment and Chemical Engineering, Heilongjiang University of Science and Technology, Harbin 150022, China, emails: lilixin1980@163.com (L. Li), shengtaofire@163.com (T. Sheng), llx8003@gmail.com (C. Sun), lilixin1980@126.com (W. Liu)*
[b]*Longjiang Environmental Protection Group Co. Ltd., Harbin, Heilongjiang 150050, email: 18567699@qq.com*
[c]*State Key Lab of Urban Water Resource and Environment, Harbin Institute of Technology, Harbin 150090, China, email: mafang@hit.edu.cn*

Received 12 May 2019; Accepted 22 October 2019

ABSTRACT

This study presents the preparation of a novel inorganic-biological composite flocculant, termed PAFC-CBF, which is composed of polymeric aluminum ferric chloride (PAFC) and compound bioflocculant (CBF). It was investigated under different PAFC/CBF weight ratios. The turbidity and total organic carbon (TOC) removal efficiency were also investigated, when PAFC-CBF was added to the surface water. Fourier-transform infrared spectroscopy, X-ray diffraction and scanning electron microscopy were performed to characterize PAFC-CBF. Finally, floc properties including floc strength and recoverability were investigated using Mastersizer 2000. The results of the investigation indicated that CBF was successfully embedded into PAFC, forming a novel flocculant with the characteristic structure of PAFC and CBF. Considering the flocculation efficiency and economic cost, PAFC-CBF demonstrated a superior flocculation performance at the flocculant dosage of 25 mg/L, with an optimal turbidity removal efficiency of 90.28%, and a TOC removal efficiency of 26.75%. During the flocculation process, charge neutralization, adsorption bridging and sweep mechanisms served in the main role of colloidal destabilization and aggregation.

Keywords: Composite flocculant; Compound bioflocculant (CBF); Polymeric aluminum ferric chloride (PAFC); Surface water treatment

1. Introduction

Flocculants are useful in the aggregation of colloids, particles, cells and suspended solids, as well as for the removal of natural organic matters from water [1]. They are commonly used in drinking water treatments, wastewater treatments and fermentation processes. Over previous decades, aluminum coagulants and organic polymer flocculants have been widely used in water treatment processes, owing to their high efficiencies and low costs, however, their use has brought about a series of health and environmental problems [2,3]. It has been reported that residual aluminum may be associated with Alzheimer's disease, while the monomer of polyacrylamide may have a poisonous effect on the nervous system [3]. By contrast, bioflocculants, which are extracellular biopolymeric substances secreted by bacteria, fungi, algae and yeast, are biodegradable and nontoxic flocculants [4,5].

Bioflocculants are attracting increasing attention in the field of flocculation research, due to the fact that they are biodegradable, non-toxic and free of secondary pollution. Bioflocculants have significant potential for industrial applications, however, the low flocculating capacity, low yield and high costs in producing bioflocculants, limits their application in water treatments [6,7]. Therefore, in order to extend the application of bioflocculants, researchers have begun to use them in combination with conventional

* Corresponding authors.

coagulants for water treatments [8]. Composite flocculants could serve as an alternative that combines the advantages of aluminum-based coagulants and bioflocculants, while reducing the dosage of aluminum coagulants and bioflocculants. In addition, the health risks associated with aluminum use can be reduced, and a large yield of bioflocculants is not required [9]. Yang et al. [10] have observed that using the bioflocculant MBFGA1 in combination with polyaluminum chloride (PAC) could not only enhance the coagulation efficiency but also reduce the PAC dosage required in kaolin suspension treatments. Furthermore, the combination of aluminum-based coagulants and bioflocculants could improve dissolved organic carbon removal and floc properties [3,9]. Li et al. [7] investigated the use of compound bioflocculants (CBFs) and PAC in kaolin-humic acid coagulation. Huang et al. [8] also studied the effects of CBFs as a coagulation aid with aluminum sulfate (AS), and PAC on coagulation performance and floc properties for dye removal. Zhang et al. [11] investigated the enhanced effects and mechanisms of CBFs and $AlCl_3$ on enhancing *Chlorella regularis* harvesting, while Ni et al. [12] compared the efficacy of both dual-coagulation and a composite coagulant of PAC and CBF in kaolin suspension treatments. Additional equipment is still required for handling dual-coagulants, which are derived from separate reagents. However, there are a limited number of studies that have examined the effect of the flocculant dosage on turbidity removal and organic matter removal in surface water treatments, by applying dual-coagulations [9]. Besides, bioflocculants are mainly made up of polysaccharide. There are some concerns about the increasing levels of organic matter when adding an amount of bioflocculants in wastewater or surface water [9]. Therefore, bioflocculants can be used as a coagulation aid in water treatment with aluminum coagulants and prepared as an inorganic-biological composite flocculant. This could be an alternative to eliminate any public health concerns. The inorganic-biological composite flocculant combines the advantages of both aluminum coagulants and bioflocculant. Moreover, dual-coagulants can reduce the necessary dosage of aluminum coagulants and bioflocculants [13].

In the present study, a novel inorganic-biological composite flocculant was prepared using the cationic inorganic reagent, PAFC, and the amphoteric organic reagent, CBF, under different PAFC/CBF weight ratios (Wr). The characterization of the constructed composite flocculant was investigated using Fourier-transform infrared (FTIR) spectroscopy, X-ray diffraction (XRD) and scanning electron microscopy (SEM). The turbidity, total organic carbon (TOC) removal efficiency and floc properties were investigated when PAFC-CBF was added to the surface water. In addition, flocculating mechanisms of composite flocculants were also explored. This novel flocculant approach is seeking to identify an efficient, environmental friendly and economical method for surface water treatment.

2. Materials and methods

2.1. Flocculants

PAFC (Al_2O_3 = 30.4%, Fe_2O_3 = 1.5%) was purchased from Harbin Xinquan Water Purification Materials Corporation, China. CBF was produced using a mixed culture of *Rhizobium radiobacter* F2 and *Bacillus sphaericus* F6, which was obtained from the State Key Laboratory of Urban Water Resource and Environment, Harbin Institute of Technology, China. CBF was mainly composed of polysaccharide (90.6%) and protein (9.3%), and had a molecular weight of 10^5–10^6 Da [14,15].

2.2. Raw water

Source water for the water treatment tests was collected from the Songhua River (located in the upstream of Harbin, China). The quality indexes of the source water were as follows: temperature, 14.2°C ± 1°C; pH, 7.1 ± 0.2; turbidity, 26.3 ± 1.5 NTU; and TOC, 6.09 ± 0.1 mg/L.

2.3. Procedure for the preparation of composite bioflocculant

Composite bioflocculant was prepared under different PAFC/CBF ratios (m/m, varying from 10 to 30). For the polymerization, the appropriate amount of PAFC powder (0.5, 1.0 and 1.5 g, respectively) was slowly added to 1 L deionized water under magnetic stirring. Then, 0.05 g of CBF powder was slowly added into 0.5, 1.0 g and 1.5 g/L PAFC solution. It was then heated to 50°C–60°C under constant stirring for 60 min, until the composite bioflocculant with different PAFC/CBF weight ratios (Wr = 10, 20 and 30) was prepared. Subsequently, the product was stored at 4°C until further use. The composite bioflocculant is denoted as PAFC-CBF.

2.4. Jar test

Flocculation experiments were performed on surface water at room temperature. All flocculation tests were conducted in 1.0 L beakers using a six-unit stirring system, and each experiment was repeated three times. Initially, water samples (1.0 L) were stirred at 200 rpm for 10 s, and then the flocculant, which ranged from 5 to 30 mg, was added to the raw water. The solution was first stirred at 200 rpm for 30 s, then at 60 rpm for 2 min, and it finally settled after 20 min [1]. At the end of each jar test, supernatant samples were withdrawn using a syringe from about 2 cm below the water surface for measurement. An unfiltered sample was used for turbidity and TOC measurements using a turbidimeter (Turb 555 IR; WTW, Germany), and a TOC analyzer (TOC-VCPH; Shimadzu, Japan), respectively. Subsequently, the removal efficiency was calculated as follows: removal efficiency (%) = $(C_0 - C)/C_0 \times 100$, where C_0 is the initial value and C is the value of the flocculation treatment.

During the flocculation process, CBF was first added at the start of rapid mixing, followed by PAFC added after 30 s. This dual-coagulant was denoted as CBF + PAFC (CBF/PAFC Wr = 1/20).

2.5. Structure and morphology

To obtain the dried powder, PAFC-CBF samples were placed in beakers and dried in a vacuum at 40°C for 1 d [16,17]. Next, PAFC, CBF and PAFC-CBF were mixed with potassium bromide (KBr) and the respective pellet was prepared, which was suitable for analysis using an FTIR spectrophotometer (SPECTRUM ONE, PerkinElmer, USA). The spectrum was measured in the range of 4,000–400 cm^{-1}. XRD

patterns of the flocculant powder were also recorded on an X-ray diffractometer (D8 ADVANCE, Bruker AXS GmbH, Germany) for the determination of the crystalline phases with Cu K radiation in the range of 5°–70° (2θ), and at a scan rate of 4°/min. Finally, a SEM device (S-4700; HITACHI, Japan) was used to investigate the structure and morphology of CBF and PAFC-CBF.

2.6. Floc strength and floc recovery

Flocs properties tests were conducted with a jar tester as mentioned above. However, after the slow stir phase completed, the shear rate suddenly increased to 200 rpm for 30 s to break up the flocs, and then back to 60 rpm for 14.5 min for the flocs to regrow. Dynamic flocs size was monitored by a laser diffraction instrument (Malvern Mastersizer2000, Malvern, UK) as the coagulation process proceeded. The suspension was monitored by drawing water through the test cell of the Mastersizer and back into the jar by a peristaltic pump on the return tube, using a 5 mm internal diameter tubing at a flow rate of 4.5 L/h. The inflow and outflow tubes were placed opposite one another at a depth just above the impeller in the holding ports. Size measurements were taken every 20 s and logged onto a personal computer (PC) [2,9].

Breakage factor (B_f), floc strength factor (S_f), and the recovery factor (R_f), which are used to compare the relative breakage and regrowth of flocs in different flocculated systems, are calculated as follows [13,14]:

$$\text{Strength factor } (S_f) = \frac{d_2}{d_1} \times 100\% \quad (1)$$

$$\text{Breakage factor } (B_f) = \frac{d_1 - d_2}{d_1} \times 100\% \quad (2)$$

$$\text{Recovery factor } (R_f) = \frac{d_3 - d_2}{d_1 - d_2} \times 100\% \quad (3)$$

where d_1 is the average floc size of the steady phase before breakage, d_2 is the floc size after breakage, and d_3 is the floc size of the new steady phase after regrowth. Flocs with a larger value of strength factor, or a lower value of breakage factor, are more resistant to ruptures. Flocs with larger recovery factors show better recoverability after a high shear. That is, it has better regrowth after breakages [13,14].

3. Results and discussion

3.1. Effect of PAFC/CBF Wr on turbidity removal

The effect of different PAFC-CBF (Wr = 10, 20 and 30) dosages vary between 5 and 30 mg/L on the turbidity removal efficiency, compared with separate CBF and PAFC effects. This is shown in Fig. 1. When the PAFC dosage was 5 mg/L, PAFC had the lowest turbidity removal efficiency. However, CBF had a higher turbidity removal efficiency than others at 5 mg/L. It was observed that the turbidity removal efficiency increased along with the increase in the dosage of CBF and it reached a maximum of 58.53% at a dosage of 25 mg/L among the singular CBF experiments. Then, the turbidity removal

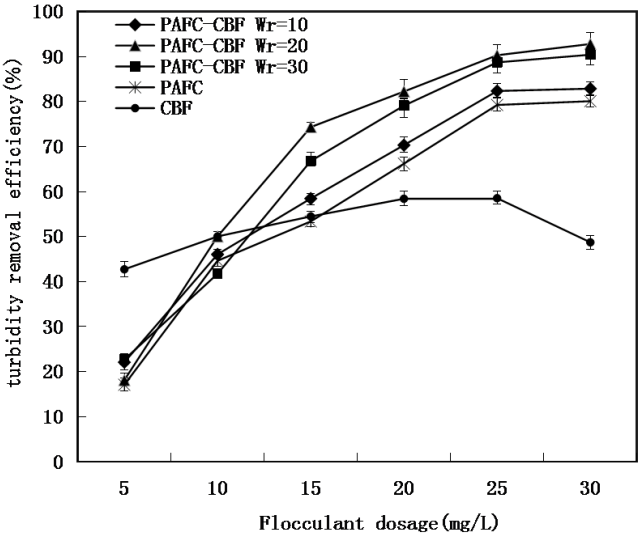

Fig. 1. Effect of PAFC/CBF weight ratios on turbidity removal.

efficiency decreased along with an increase in the dosage of CBF. It was observed that the turbidity removal efficiency increased along with the increase in the dosage of PAFC, and reached a maximum of 88.02% at a dosage of 30 mg/L, among the PAFC experiments. Moreover, the combined PAFC-CBF experiment exhibited higher turbidity removal efficiency compared with the separate PAFC and CBF tests. The PAFC-CBF dosage to achieve the highest removal efficiency of 92.78% was reported to be at the flocculant dosage of 30 mg/L, and the turbidity was at 1.82 NTU.

At a Wr between 10 and 30, the turbidity of PAFC-CBF was lower than that of PAFC, with a dosage ranging between 15 and 30 mg/L. In addition, the turbidity initially decreased and then increased with an increasing Wr at the same flocculant dosage. PAFC-CBF with Wr = 20 was more efficient compared with flocculants with other Wr, or with PAFC in terms of the turbidity removal under the dosage of 15–30 mg/L. When the dosage of PAFC-CBF with Wr = 20 was 30 mg/L, the turbidity was the lowest, at 1.82 NTU, and the removal efficiency of turbidity was 92.78%. The results indicate that charge neutralization was a significant flocculation mechanism by the composite flocculant [12]. Furthermore, it was suspected that the adsorption and bridging effect of CBF performed a positive role in the removal of turbidity [18]. The results of these experiments were aligned with findings in previous studies [2,13]. The obtained actual turbidity removal efficiency at the PAFC-CBF dosage of 20 mg/L was close to that at the 30 mg/L dosage of just the PAFC. Considering the flocculation efficiency and economic cost, the optimal dosage of PFAC-CBF was 25 mg/L, and a turbidity removal efficiency of 90.28% could be achieved.

3.2. Effect of PAFC/CBF Wr on TOC removal

As shown in Fig. 2, the TOC removal efficiency of PAFC-CBF with Wr = 10 first increased and then decreased, with an increase of the dosage. This is mainly due to the fact that PAFC-CBF with Wr = 10 have more polysaccharides [1]. When the dosage of PAFC-CBF was over 25 mg/L, an

excessive introduction of polysaccharides resulted in a low removal efficiency of TOC. In the PAFC-CBF with Wr = 20 and PAFC-CBF with Wr = 30 experiment groups, the removal rate of TOC increased, with an increase of the dosage. When the dosage of the flocculant was the same, the TOC removal efficiency of PAFC-CBF with Wr = 20 was higher, than that of PAFC-CBF with Wr = 30.

As shown in Fig. 2, the TOC removal efficiency of PAFC-CBF displayed a similar trend to that of PAFC, demonstrating an increase in TOC removal efficiency as the flocculant dosage increased. When the PAFC-CBF dosage was lower than 25 mg/L, PAFC-CBF showed better TOC removal efficiency than PAFC, while PAFC performed better when the flocculant dosage was higher than 25 mg/L. The maximum TOC removal efficiency of 30.86% was obtained at the PAFC dosage of 30 mg/L. There was little difference between PAFC and PAFC-CBF in terms of TOC removal efficiency, under the same dosage at values higher than 25 mg/L. Direct formation of aggregates with the particles in surface water was difficult for CBF and might result in an increase of the repulsion between particles due to its negative charge. Additionally, it would increase the burden of PAFC as a type of organic matter [9]. However, adding CBF into PAFC could enhance the flocculation performance due to the additional bridging bonds between CBF and Al/Fe-particles. Thus, the aforementioned results reveal that PAFC-CBF not only possessed an excellent flocculation performance in TOC removal, but it could also effectively avoid the source water pollution of the organic matter, when CBF as part of the PAFC-CBF was added to the source water.

3.3. FTIR, XRD and SEM analyses

3.3.1. FTIR analysis

The possible chemical bonds in PAFC-CBF, PAFC and CBF were investigated by examining the FTIR characteristic peaks in the range of 4,000–400 cm^{-1}, to match the corresponding chemical bonds. The PAFC-CBF, PAFC and CBF samples were dried and pressed into pellets along with potassium bromide (KBr) for FTIR studies. The FTIR spectra of PAFC-CBF, PAFC and CBF are shown in Fig. 3.

The spectrum of CBF displayed a broad stretching peak at 3,443 cm^{-1}, which is characteristic of the hydroxyl and amino groups [19,20]. A weak C–H asymmetric stretching vibration band was observed at 2,926 cm^{-1} [19,20]. The peaks at 1,654 cm^{-1} represented the presence of carbonyl groups, which was characteristic of C=O in an amide group [18,20]. The strong absorption at 1,116 cm^{-1} indicated the C–O stretching vibration and the presence of methoxyl groups [20,21]. These bands could be an indication of polysaccharide and its derivatives in CBF [12,18]. In addition, the absorption peak of C–H at 860 cm^{-1} is known to be characteristic of mannoside, which indicated that CBF contained β-configuration in its structure. The infrared spectrum of CBF evidenced the presence of carboxyl, hydroxyl and amino groups. These functional groups, which could serve as binding sites for the cations, as well as for suspended particles, were the preferred groups for most of the adsorption processes [18].

The spectrum of PAFC demonstrated a broad absorption peak in the range of 3,300–3,600 cm^{-1}, which was due to the stretching vibration of –OH groups, as displayed in Fig. 3 [16,22]. The medium peak in the range of 1,600–1,700 cm^{-1} (1,630 cm^{-1} for PAFC) was assigned to the bending vibration of –OH groups in the water molecule, namely the H–O–H angle distortion frequency, indicating that PAFC might contain structural and adsorbed water [16,22]. Also, there was a sharp adsorption peak at 960 cm^{-1} in the PAFC spectrum, which might be assigned to the Al–O–Al bond stretching and bending vibrations at these frequencies.

As seen in Fig. 3, the PAFC-CBF spectrum displayed almost the same characteristic bands as pure PAFC, with the exception of the peaks at 3,430, 1,116 and 860 cm^{-1}. There was a significant difference in the spectra of PAFC-CBF and PAFC at wavenumbers of 3,300–3,600 cm^{-1}. The FTIR spectrum of PAFC demonstrated two obvious bands in the range of 3,300–3,600 cm^{-1}, which were due to the O–H stretching vibration, including free hydroxyl and associating hydroxyl stretching vibrations. However, the FTIR spectrum of PAFC-CBF presented a broad absorption peak in the range of

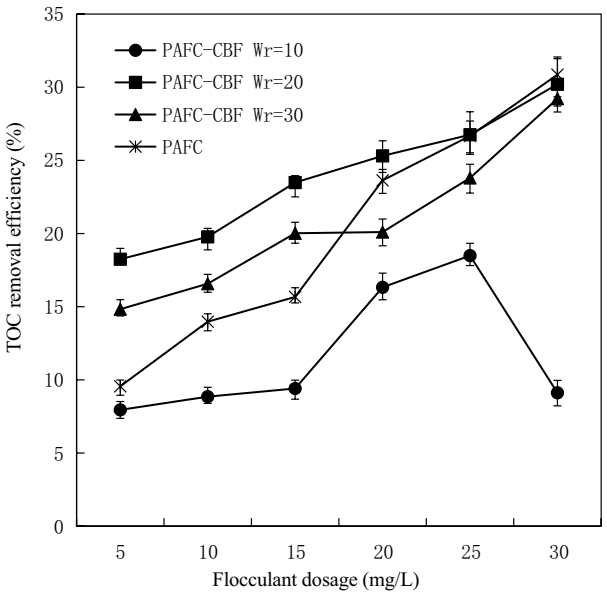

Fig. 2. Effect of PAFC/CBF weight ratios on TOC removal.

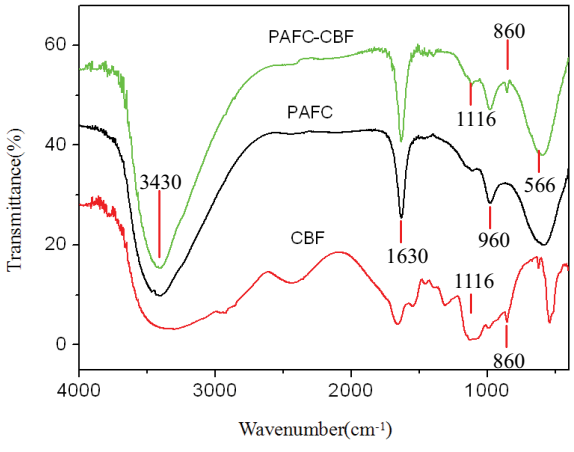

Fig. 3. FTIR spectra of PAFC-CBF, PAFC and CBF.

3,300–3,600 cm^{-1}. Compared with the FTIR spectrum of PAFC, the broad absorption peak of PAFC-CBF indicated that the associating degree of the hydroxyl groups was higher and the stability of PAFC-CBF was better. The bands at 1,116 and 860 cm^{-1} were assigned to the stretching vibrations of C–O and C–H, which are characteristic of mannoside, and these were only present in CBF [18]. These results further confirmed the incorporation of CBF groups onto the backbone of PAFC, and that PAFC-CBF was an inorganic-biological composite flocculant. Regarding the changes occurring in the spectrum of PAFC-CBF, it could be noticed that they were similar to those observed in the case of PAFC. Due to the relatively small amount of CBF in PAFC-CBF, there was a small difference between the FTIR spectra of PAFC-CBF and that of CBF. The infrared spectrum of PAFC-CBF evidenced the presence of carboxyl, hydroxyl, Al–O and other groups. These functional groups were the preferred groups for most adsorption processes [18], which supplied sufficient adsorption sites for particles in the flocculation process. Meanwhile, Fe and Al could be easily hydrolyzed to enhance the flocculation efficiency.

3.3.2. XRD analysis

Fig. 4 presents the XRD spectra of PAFC, CBF and PAFC-CBF. The XRD pattern of PAFC in Fig. 4a demonstrated that the diffraction intensity curve was disorderly and nearly smooth, while the peaks of iron, aluminum and their compounds were not observed. The Fe–Al hydroxy copolymer in PAFC showed a disordered state, indicating that PAFC existed in an amorphous structure [23]. In Fig. 4b, the diffraction angles of the CBF characteristic peaks were observed to be 31.96°, 45.66°, 56.64°and 66.4°. These characteristic peaks of CBF also existed in the XRD pattern of PAFC-CBF in Fig. 4c, and it was observed that the peak of Fe_2O_3 with the diffraction angle of 32.80° appeared. These results indicated that the ferric ions in PAFC underwent hydrolytic oxidation during the PAFC-CBF preparation process, while iron, aluminum and other materials of PAFC were successfully combined with CBF. Compared with the XRD pattern of CBF, it was found that the diffraction intensities of the PAFC-CBF pattern were reduced and in the range of 31.84°–66.30°. This could be attributed to the new chemical bonds formed between PAFC and CBF, suggesting that a new flocculant was formed. This result was also consistent with the findings of the infrared analysis. In comparison with CBF, the diffraction peaks of the PAFC-CBF slightly shifted to lower diffraction angles, demonstrating that CBF fully intercalated PAFC, and the new composite flocculant was successfully prepared [24].

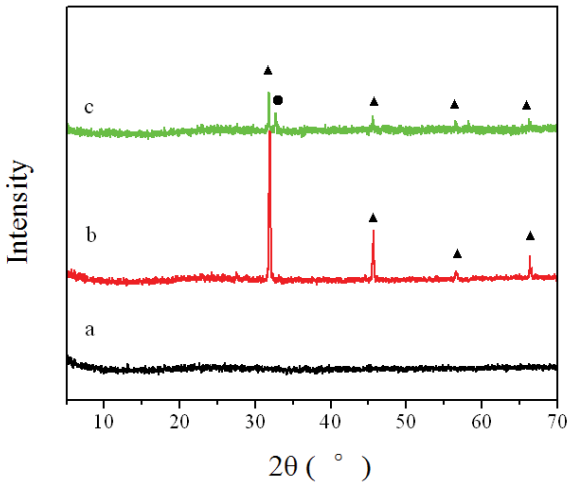

Fig. 4. XRD patterns of (a) PAFC, (b) CBF and (c) PAFC-CBF.

3.3.3. SEM analysis

SEM was used to investigate the surface morphology of CBF and PAFC-CBF, and the results are presented in Fig. 5. As observed in Fig. 5a, it was evident that CBF showed an entangled polymolecular structure. An amorphous structure was observed at the same time, which was different from the crystal-linear structure of the bioflocculant TJ-F1 [25]. This structure of the CBF had a high specific surface area, while simultaneously providing sufficient binding adsorption sites for pollutants, thus creating a favorable spatial structure for adsorption.

As shown in Fig. 5b, it was clear that PAFC-CBF displayed a different surface morphology from that of CBF in Fig. 5a. The surface of PAFC-CBF consisted of irregular, porous and distinguishable needle cluster formations with a series of pleated ditches of different widths and depths, resulting in a much coarser surface and larger specific surface area compared with CBF. This structure might be caused by CBF filling the skeleton structure of PAFC. In addition, it indicated that there was a crosslinked structure between PAFC and CBF, which could enhance the adsorption and sweep of PAFC-CBF. The molecular chains of the components in PAFC-CBF were connected to form a network structure, promoting the adsorption and bridging performance of PAFC-CBF as a flocculant. The rough surface area and the protruding area increased the surface energy and the adsorption area of PAFC-CBF, leading to richer binding sites for pollutants than CBF and an enhanced adsorption performance. It could be inferred that PAFC-CBF was favorable for the adsorption of pollutants due to its unique structure.

The conclusions drawn are based on previous studies which indicated that, due to the addition of CBF with a great number of negatively charged groups during the preparation process, PAFC was a cationic flocculant with more positive charges. PAFC and CBF were most likely to adsorb each other by the electrostatic force, and CBF was wrapped on the surface of PAFC to form a new composite flocculant. However, the formation mechanism requires further research.

3.4. Floc strength and floc recovery

After the formation stage, the formed flocs broke into small pieces under a high shear rate. When the slow shear rate was restored, aggregates regrew but could not reach their primary size. The flocs ability to resist high shear force can be indicated by both the strength factor (Eq. (1)) and the breakage factor (Eq. (2)). The flocs ability to recover after breakages can be indicated by a recovery factor (Eq. (3)). Higher strength factors and lower breakage factors reflect that flocs were more resistant to a high share rate. Moreover, higher recovery factors reflect that flocs were more recoverable. The

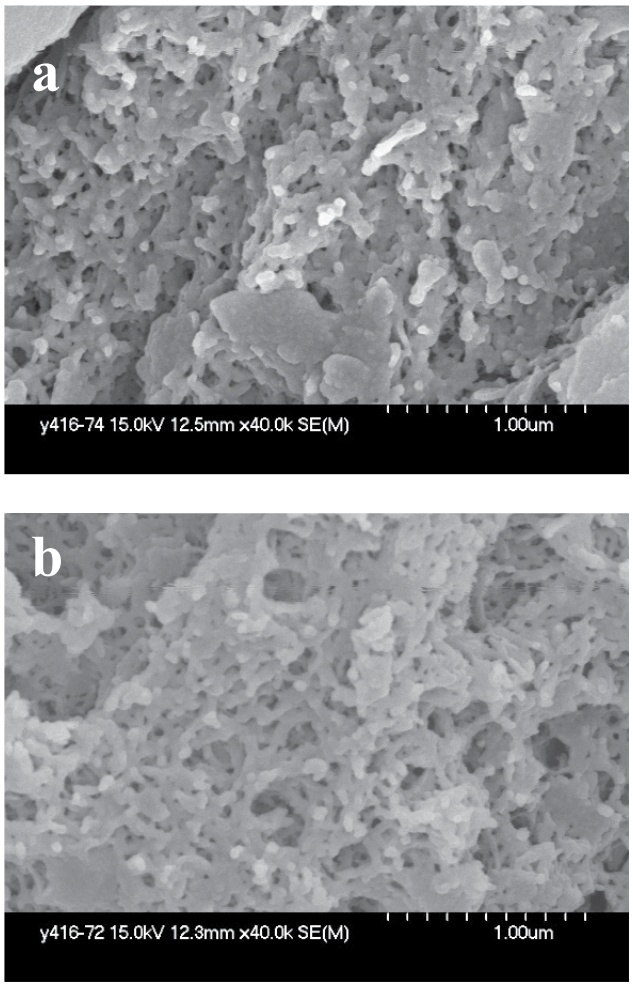

Fig. 5. SEM micrographs of (a) CBF and (b) PAFC-CBF

effect of dosing PAFC alone and PAFC-CBF was shown in Table 1, respectively. It was obvious that different flocculants resulted in different strengths, breakages and recovery factors.

The floc strength factor of PAFC was higher than the floc strength factor of PAFC-CBF. In contrast, the recovery factor was lower than that of the latter. This indicates that reformation hardly occurred. The flocs of PAFC had a higher strength and were not easy to break, but the recovery ability of the floc breakage was less than that of the floc breakage for PAFC-CBF. The results showed that the flocs strength of PAFC-CBF was slightly lower than that of PAFC, but the broken flocs easily recover and regrow. The maximum recovery factor PAFC-CBF was 84.11%, while the recovery factor of PAFC was only 68.90%. For the flocs of PAFC, the strength factor was 46.25%, which was difficult to recover after the floc breakage. The results indicated that the floc recoverability was improved by CBF [14]. Flocs were broken immediately when the high shear rate was introduced. Simultaneously, the bioflocculant chains may undergo scissions under such conditions, and the adsorbed biopolymer could reform on the particle surface [13]. As a result, new adsorption sites may come into being to bind the broken flocs together [13].

Table 1
Breakage factor, strength factor and recovery factor of PAFC-CBF

	Strength factor	Breakage factor	Recovery factor
PAFC	46.25%	53.75%	68.90%
PAFC-CBF	44.73%	55.27%	84.11%

3.5. Flocculation mechanisms of PAFC-CBF

In general, the floc formation process can be divided into two stages: first, the flocculant is added to the water. The colloids are quickly destabilized and form "micro-floc". Subsequently, more collisions occur between micro-flocs allowing faster aggregation. Finally, the larger flocs rapidly precipitate. This suggests that the polymer could be adsorbed onto the surface of colloids in the water with its long chains, where the tails and loops are extended far beyond its surface, and they can then interact with other particles via bridging flocculation [26].

In the present study, the zeta potentials of colloids in the surface water, CBF and PAFC-CBF were –25.2 ± 1.25, –30.6 ± 1.35 and –13.0 ± 1.18 mV, respectively. This suggests that the charge neutralization is not the only mechanism for the PAFC-CBF. When PAFC-CBF was added to the water sample, the PAFC-particle micro-complex was formed. The stable colloids were effectively destabilized throughout the charge neutralization and efficient collisions, which led to an increase of aggregation during the initial aggregation [13]. Then, these destabilized the PAFC-particle micro-complex, which aggregated to larger flocs by the bridging of the bioflocculant chains with lots of branched structures [2,9]. As a result, the turbidity and TOC were efficiently removed by the combined action of PAFC and CBF. The action of PAFC was conducted through neutralizing the negative charge on the surface of the colloids, which reduced the electrostatic repulsion and shortened the distance between the colloids [7,11]. In general, the inorganic chemical flocculants displaced the positive charge and therefore enabled the aggregation of the colloids. Since the distance was shortened to some extent, CBF began to patch and formed bridges between the micro-aggregates, making them form larger flocs. The larger flocs then rapidly precipitated [9,13]. The flocculation process used in this study is described in Fig. 6.

As mentioned above, higher turbidity and TOC removal efficiency were obtained, where the coagulation mechanism could be a combination of charge neutralization, adsorption bridging and sweep mechanisms in the presence of CBF, in comparison with PAFC alone. The trends of turbidity and TOC removal efficiency of PAFC-CBF were almost the same as those of PAFC, which indicated that PAFC played an important role in PAFC-CBF, as mentioned earlier. Accordingly, charge neutralization was very likely to be the dominant flocculation mechanism for PAFC-CBF. However, PAFC-CBF causes the flocculation of particles by charge neutralization, sweep and adsorption bridging. Regardless of which mechanism would be dominant in flocculation, it can be assumed that bridging eventually occurred after the particles had adsorbed onto the chains of PAFC-CBF [12].

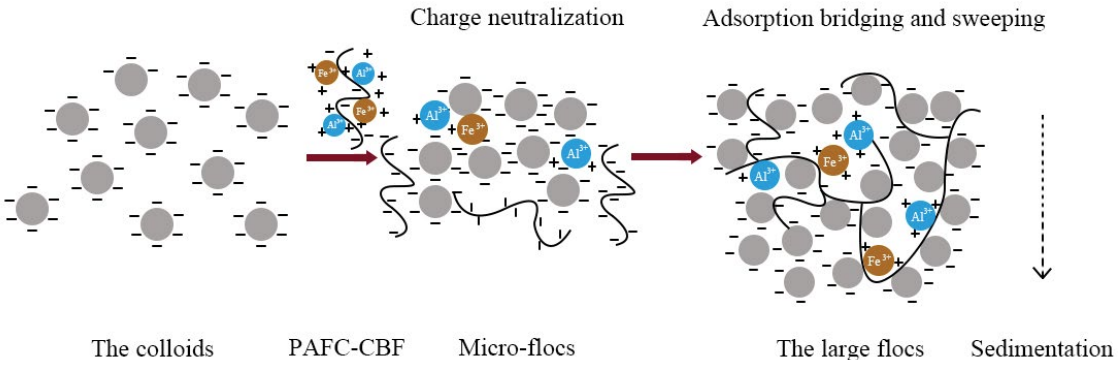

Fig. 6. Flocculation mechanisms of PAFC-CBF.

4. Conclusions

A novel inorganic-biological composite flocculant, PAFC-CBF, which is composed of polymeric aluminum ferric chloride (PAFC) and CBF was synthesized. The success of the PAFC-CBF was confirmed by FTIR, XRD and SEM characterization. The turbidity and TOC removal efficiency of PAFC-CBF under different PAFC/CBF weight ratios were evaluated in the surface water treatment. Finally, floc properties including floc strength and recoverability were investigated by Mastersizer 2000. The results indicated that PAFC-CBF exhibited much higher flocculating capability in the surface water treatment as compared with PAFC alone and CBF alone. The flocs recovery ability was improved by adding PAFC-CBF in comparison of PAFC alone. Considering the flocculation efficiency and economic cost, the optimum PAFC-CBF dosage was 25 mg/L, while turbidity and TOC removal efficiencies of 90.28% and 26.75% could be achieved, respectively. It could be concluded that charge neutralization, adsorption bridging and sweep mechanisms were involved in the flocculation process of PAFC-CBF. Furthermore, the charge neutralization was very likely to be the dominant flocculation mechanism for PAFC-CBF. Therefore, all of the results presented above affirmed the potential of PAFC-CBF in the source water treatment field.

Acknowledgments

The work is supported by grants from National Natural Science Foundation of China (No. 51678222 and 51408200), China Scholarship Council (No. 201508230084), Open Project of State Key Laboratory of Urban Water Resource and Environment-Harbin Institute of Technology (No. ES201803), The China Postdoctoral Science Foundation (No. 2018M641888) and The promising Youngsters Training Program of Heilongjiang University of Science and Technology (No. Q20120201).

References

[1] L.X. Li, F. Ma, H.M. Zuo, Production of a novel bioflocculant and its flocculation performance in aluminum removal, Bioengineered, 7 (2016) 98–105.
[2] X.W. Bo, B.Y. Gao, N.N. Peng, Y. Wang, Q.Y. Yue, Y.C. Zhao, Effect of dosing sequence and solution pH on floc properties of the compound bioflocculant–aluminum sulfate dual-coagulant in kaolin–humic acid solution treatment, Bioresour. Technol., 113 (2012) 89–96.
[3] X. Huang, S.L. Sun, B.Y. Gao, Q.Y. Yue, Y. Wang, Q. Li, Coagulation behavior and floc properties of compound bioflocculant–polyaluminum chloride dual-coagulants and polymeric aluminum in low temperature surface water treatment, J. Environ. Sci., 30 (2015) 215–222.
[4] L.X. Li, L.Y. Feng, F. Ma, Q.S. Zhao, Flocculating properties and production of the compound bioflocculant by *Rhizobium radiobacter* F2 and *Bacillus sphaeicus* F6, J. Harbin Inst. Technol. (New Ser.), 22 (2015) 20–26.
[5] L.X. Li, L.Y. Feng, F. Ma, Removal of the organic matter by combination of compound bioflocculants and polyaluminium chloride for treatment of source water, Basic Clin. Pharmacol., 119 (2016) 15–16.
[6] L.X. Li, J. Xing, F. Ma, T. Pan, Introduction of compound bioflocculant and its application in water treatment, Adv. J. Food Sci. Technol., 9 (2015) 695–700.
[7] R.H. Li, B.Y. Gao, X. Huang, H.Y. Dong, X.C. Li, Q.Y. Yue, Y. Wang, Q. Li, Compound bioflocculant and polyaluminum chloride in kaolin-humic acid coagulation: factors influencing coagulation performance and floc characteristics, Bioresour. Technol., 172 (2014) 8–15.
[8] X. Huang, X.W. Bo, Y.X. Zhao, B.Y. Gao, Y. Wang, S.L. Sun, Q.Y. Yue, Q. Li, Effects of compound bioflocculant on coagulation performance and floc properties for dye removal, Bioresour. Technol., 165 (2014) 116–121.
[9] X. Huang, B.Y. Gao, Q.Y. Yue, Y. Wang, Q. Li, S. Zhao, S.L. Sun, Effect of dosing sequence and raw water pH on coagulation performance and flocs properties using dual-coagulation of polyaluminum chloride and compound bioflocculant in low temperature surface water treatment, Chem. Eng. J., 229 (2013) 477–483.
[10] Z.H. Yang, J. Huang, G.M. Zeng, M. Ruan, C.S. Zhou, L. Li, Z.G. Rong, Optimization of flocculation conditions for kaolin suspension using the composite flocculant of MBFGA1 and PAC by response surface methodology, Bioresour. Technol., 100 (2009) 4233–4239.
[11] C.F. Zhang, X.S. Wang, Y. Wang, Y.B. Li, D.D. Zhou, Y.W. Jia, Synergistic effect and mechanisms of compound bioflocculant and $AlCl_3$ salts on enhancing *Chlorella regularis* harvesting, Appl. Microbiol. Biotechnol., 100 (2016) 5653–5660.
[12] F. Ni, X.J. Peng, J.S. He, L. Yu, J. Zhao, Z.K. Luan, Preparation and characterization of composite bioflocculants in comparison with dual-coagulants for the treatment of kaolin suspension, Chem. Eng. J., 213 (2012) 195–202.
[13] X.W. Bo, B.Y. Gao, N.N. Peng, Y. Wang, Q.Y. Yue, Y.C. Zhao, Coagulation performance and floc properties of compound bioflocculant-aluminum sulfate dual-coagulant in treating kaolin-humic acid solution, Chem. Eng. J., 173 (2011) 400–406.
[14] Y.X. Zhao, B.Y. Gao, H.K. Shon, Y. Wang, J.H. Kim, Q.Y. Yue, X.W. Bo, Anionic polymer compound bioflocculant as a coagulant aid with aluminum sulfate and titanium tetrachloride, Bioresour. Technol., 108 (2012) 45–54.

[15] X. Huang, B.Y. Gao, Q.Y. Yue, Y.Y. Zhang, S.L. Sun, Compound bioflocculant used as a coagulation aid in synthetic dye wastewater treatment: the effect of solution pH, Sep. Purif. Technol., 154 (2015) 108–114.
[16] G.C. Zhu, H.L. Zheng, Z. Zhang, T. Tshukudu, P. Zhang, X.Y. Xiang, Characterization and coagulation–flocculation behavior of polymeric aluminum ferric sulfate (PAFS), Chem. Eng. J., 178 (2011) 50–59.
[17] J. Zou, H. Zhu, F.H. Wang, H.Y. Sui, J.T. Fan, Preparation of a new inorganic–organic composite flocculant used in solid–liquid separation for waste drilling fluid, Chem. Eng. J., 171 (2011) 350–356.
[18] L.L. Wang, F. Ma, Y.Y. Qu, D.Z. Sun, A. Li, J.B. Guo, B. Yu, Characterization of a compound bioflocculant produced by mixed culture of *Rhizobium radiobacter* F2 and *Bacillus sphaeicus* F6, World J. Microbiol. Biotechnol., 27 (2011) 2559–2565.
[19] X.H. Zhang, J. Sun, X.X. Liu, J.T. Zhou, Production and flocculating performance of sludge bioflocculant from biological sludge, Bioresour. Technol., 146 (2013) 51–56.
[20] Y.J. Yin, Z.M. Tian, W. Tang, L. Li, L.Y. Song, S.P. Mcelmurry, Production and characterization of high efficiency bioflocculant isolated from *Klebsiella* sp. ZZ-3, Bioresour. Technol., 171 (2014) 336–342.
[21] Z. Li, S. Zhong, H.Y. Lei, R.W. Chen, Q. Yu, H.L. Li, Production of a novel bioflocculant by *Bacillus licheniformis* X14 and its application to low temperature drinking water treatment, Bioresour. Technol., 100 (2009) 3650–3656.
[22] Y.B. Zeng, J. Park, Characterization and coagulation performance of a novel inorganic polymer coagulant—Poly-zinc-silicate-sulfate, Colloids Surf., A, 334 (2009) 147–154.
[23] C.Z. Sun, Q.Y. Yue, B.Y. Gao, B.C. Cao, R.M. Mu, Z.B. Zhang, Synthesis and floc properties of polymeric ferric aluminum chloride–polydimethyl diallylammonium chloride coagulant in coagulating humic acid–kaolin synthetic water, Chem. Eng. J., 185 (2012) 29–34.
[24] X.G. Quan, H.Y. Wang, Preparation of a novel coal gangue–polyacrylamide hybrid flocculant and its flocculation performance, Chin. J. Chem. Eng., 22 (2014) 1055–1060.
[25] S.Q. Xia, Z.Q. Zhang, X.J. Wang, A.M. Yang, L. Chen, J.F. Zhao, D. Leonard, N. Jaffrezic-Renault, Production and characterization of a bioflocculant by *Proteus mirabilis* TJ-1, Bioresour. Technol., 99 (2008) 6520–6527.
[26] Y.L. Luo, Z.H. Yang, Z.Y. Xu, L.J. Zhou, G.M. Zeng, J. Huang, Y. Xiao, L.K. Wang, Effect of trace amounts of polyacrylamide (PAM) on long-term performance of activated sludge, J. Hazard. Mater., 189 (2011) 69–75.